

# Synthesis, Structure, and Properties of Sodium or Potassium-Doped Lanthanum Orthomanganites from NaCl or KCl Flux<sup>1</sup>

Ram Niwas Singh,\* C. Shivakumara,\* N. Y. Vasanthacharya,\* S. Subramanian,† M. S. Hegde,\*  
H. Rajagopal,‡ and A. Sequeira‡

\*Solid State and Structural Chemistry Unit, and †Department of Metallurgy, Indian Institute of Science, Bangalore 560 012, India; and

‡Solid State Physics Division, Bhabha Atomic Research Center, Trombay, Mumbai 400 085, India

Received February 2, 1997; in revised form October 6, 1997; accepted October 9, 1997

Lanthanum and oxygen-deficient  $\text{La}_{1-x-y}\text{A}_x\text{MnO}_{3-\delta}$  ( $\text{A} = \text{Na}$  or  $\text{K}$ ) ferromagnetic oxide phases have been synthesized from NaCl or KCl flux, starting from  $\text{La}_2\text{O}_3$  and  $\text{MnCO}_3$  at  $900^\circ\text{C}$ . Composition of the final product could be varied by varying initial composition  $\text{La}_y\text{MnO}_3$  ( $0.7 < y < 1$ ). Final composition of these oxides was obtained from chemical analysis of elements present. As the lanthanum content increased, Na or K content decreased and the structure changed from rhombohedral to orthorhombic symmetry.  $\text{Mn}^{4+}$  concentration was 27% in the sodium doped manganite,  $\text{La}_{0.82}\text{Na}_{0.13}\text{MnO}_{2.93}$  with Curie temperature 325 K, and  $\text{Mn}^{4+}$  was 25% in the potassium doped  $\text{La}_{0.82}\text{K}_{0.08}\text{MnO}_{2.89}$  with  $T_c$  of 310 K. Structure of these two phases have been refined from neutron diffraction studies. Stoichiometric  $\text{La}_{1-x}\text{A}_x\text{MnO}_3$  ( $\text{A} = \text{Na}$  or  $\text{K}$ ) have been obtained for the initial composition  $\text{La}_y\text{MnO}_3$  ( $y = 0.85$ ). Orthorhombic phases obtained were found to be Mn-deficient  $\text{La}_{1-x}\text{Na}_x\text{Mn}_{1-x}\text{Mn}_{1-y}\text{O}_3$  ( $x \approx 0.02$ ;  $y \approx 0.05$ ), which were ferromagnetic insulators, even though total  $\text{Mn}^{4+}$  contents were as high as 29%.

© 1998 Academic Press

## 1. INTRODUCTION

Lanthanum orthomanganites of general formula  $\text{La}_{1-x}\text{A}_x\text{MnO}_3$  ( $\text{A} = \text{Ca}$ ,  $\text{Sr}$ ,  $\text{Ba}$ , and  $\text{Pb}$ ) have been known for a long time (1, 2). Recent observation of colossal magnetoresistance ( $\text{CMR} = (R_H - R_0)/R_0$ ) in  $\text{La}_{1-x}\text{A}_x\text{MnO}_3$  has generated new interest in these materials (3–6). Exact reason for CMR is a subject of current interest (7, 8). It is desirable to have CMR at 300 K for commercial application. Highest CMR is observed near the ferromagnetic transition temperature  $T_c$ , and hence the search for new materials having  $T_c$  near 300 K. Goodenough (9) has indicated that  $\text{La}_y\text{MnO}_3$  ( $y < 1$ ) showed  $T_c$  165–220 K. Recently we had shown that a  $T_c$  of 220 K is obtained in the bulk solid as well as thin films of lanthanum-deficient oxide

having nominal composition  $\text{La}_{0.76}\text{MnO}_{2.86}$  (10). Further, films of such material showed over 80% CMR at 220 K at 6.5 T. Oxygen ion deficiency in  $\text{La}_{0.67}\text{Ba}_{0.33}\text{MnO}_{3-\delta}$  and  $\text{La}_{0.6}\text{Pb}_{0.4}\text{MnO}_{3-\delta}$  showed a decrease in  $T_c$ , but there is an increase in CMR (11, 12). Cation as well as anion deficiency is likely to be one of the reasons for such a large CMR in  $\text{La}_y\text{MnO}_{3-\delta}$  ( $y < 1$ ). Solid state preparation of  $\text{La}_y\text{MnO}_3$  invariably gave multiphase mixtures with  $\text{Mn}_3\text{O}_4$  as an impurity. In an attempt to eliminate the  $\text{Mn}_3\text{O}_4$  impurity via water soluble manganese salts, synthesis of lanthanum-deficient phases were attempted using neutral NaCl and KCl fluxes. Since Na or K can substitute for La (13), we obtained ferromagnetic Na or K doped lanthanum manganites. Among the large number of Na or K doped lanthanum manganites synthesized by this method, epitaxial thin film of  $\text{La}_{0.82}\text{Na}_{0.13}\text{MnO}_{2.93}$  was made by pulsed laser deposition, and the thin film showed over 70% CMR at 290 K in 6T magnetic field (14). Composition of these phases has been derived by chemical analysis of La, Na/K, Mn, and oxygen independently. Here we report a new method to synthesize Na or K doped lanthanum orthomanganites by neutral NaCl or KCl flux. Structure, electrical, and magnetic properties of these oxides have been presented.

## 2. EXPERIMENTAL

$\text{La}_2\text{O}_3$  and  $\text{MnCO}_3$  for a starting composition  $\text{La}_y\text{MnO}_3$  ( $0.6 < y < 1$ ) were mixed with dry NaCl in the weight ratio 1:16. The mixture was heated to  $900^\circ\text{C}$  for 24 h in an alumina crucible. The melt was furnace cooled and washed in hot, distilled water until no  $\text{Na}^+$  or  $\text{Cl}^-$  was detected in the filtrate. The black solid was filtered and dried at  $110^\circ\text{C}$ . Similarly, a series of oxides were prepared in KCl melt. Powder X-ray diffraction (JEOL JDX-8P) patterns were recorded at a scan rate of  $2^\circ/\text{min}$  with  $\text{CuK}\alpha$  ( $1.5418 \text{ \AA}$ ). Final composition of these oxides was obtained from chemical analysis of the elements present. Neutron diffraction patterns for the two samples with starting

<sup>1</sup>Contribution 1275 from Solid State and Structural Chemistry Unit.

compositions  $\text{La}_{0.7}\text{MnO}_3$  in NaCl and KCl melt preparation were recorded at room temperature using the T-1011 diffractometer at the 100 MW Dhruva Reactor at Trombay. The samples were in the form of cylindrical pellets (10 mm in diameter and 10 mm in height), and the wavelength was 1.216 Å. The instrument collimations (FWHM) were  $0.7^\circ$ – $0.5^\circ$ – $0.7^\circ$  from the in-pile to the detector end. The patterns were analyzed by Rietveld profile refinement method using a modified version of the program DBW 3.2 (15).

In order to see the stability of these oxides and for resistivity measurements, all these oxides were sintered at  $850^\circ\text{C}$  in flowing oxygen for 24 h. Magnetic susceptibility was measured on the powder as well as the sintered samples employing a Lewis coil magnetometer with magnetic field at 1 K gauss. Four probe electrical resistivity measurements were done on the sintered pellet. Composition of the sintered samples was again determined and no significant variation in the composition was observed.

### 2.1. Lanthanum Estimation

About 0.1 g of the oxide was dissolved in 10 ml of 1:1 HCl and evaporated to dryness. The salt was dissolved in 20 ml of  $\text{H}_2\text{O}$ . To this, 20 ml of 0.1 M NaF solution was added. The solution was maintained at 5.5 pH and titrated against standard  $\text{La}(\text{NO}_3)_3$  solution using Fluoride ion sensitive electrode (ORION: expandable ion analyzer EA 940) (16).  $\text{La}(\text{NO}_3)_3$  was independently standardized by EDTA titration employing the standard  $\text{Zn}^{2+}$  ion. Accuracy of lanthanum estimation is confirmed to be better than 0.5%. There was no interference due to Mn presence at 5.5 pH.

### 2.2. Manganese Estimation

After the lanthanum estimation, the same solution was used for total manganese estimation. A quantity 150 ml of sodium pyrophosphate (10 g in 150 ml) was taken and pH was brought to  $6.7 \pm 0.2$  using a standard glass electrode. This was added to the solution containing  $\text{Mn}^{2+}$  ions. This solution was titrated against standard  $\text{KMnO}_4$  solution potentiometrically using Pt and calomel electrodes holding pH at 6.7 (17). Accuracy of Mn content is better than 0.5%. Identical experiments were carried out with pure  $\text{Mn}_3\text{O}_4$  and  $\text{MnO}_2$  samples in the presence and absence of  $\text{La}^{3+}$  ions and there is no interference of La in the estimation of Mn at pH 6.7.

### 2.3. Sodium and Potassium Estimation

Na and K contents were estimated by ICP spectroscopic technique employing a Jobin YVON analyzer. A quantity 0.5 g of the oxide was dissolved in 5 ml of 6N HCl, evaporated to dryness, and redissolved in  $\text{H}_2\text{O}$  to 50 ml. Standard solutions were prepared from analytical grade NaCl and

KCl salts dried at  $200^\circ\text{C}$ . Accuracy of estimation is better than 1%.

### 2.4. Oxygen Estimation

From the absolute weights of elements present in 1 g of an oxide, molar ratio of La:Na:Mn was determined. For example,  $\text{La}_{0.82}\text{Na}_{0.13}\text{Mn}_1\text{O}_y$  was the composition for an oxide obtained from the starting composition  $\text{La}_{0.7}\text{MnO}_3$ . The formula of this oxide can be written as  $\text{La}_{0.82}\text{Na}_{0.13}\text{Mn}_{1-x}^{3+}\text{Mn}_x^{4+}\text{O}_{2.795+x/2}$ . The value of  $x$  was estimated by iodometric titration. Typically, about 0.1 g of oxide was dropped in 10 ml of 1:1 HCl containing 2–3 g of KI. Liberated iodine was titrated against standard sodium thiosulphate solution using starch as an indicator. Compositions of each oxide was thus determined by chemical analysis of all the elements present in the compound.

## 3. RESULTS

Powder X-ray diffraction patterns of typical sodium doped lanthanum manganites are shown in Fig. 1. These melt-grown solids crystallized in perovskite related structures. For the starting composition of  $\text{La}_y\text{MnO}_3$  ( $0.7 < y < 0.9$ ), compounds crystallized in rhombohedral structure, as can be seen from Figs. 1a and 1b. All the diffraction lines could be indexed and no impurity lines due to either  $\text{La}_2\text{O}_3$  or any of the known oxides of Mn, such as  $\text{Mn}_2\text{O}_3$ ,  $\text{Mn}_3\text{O}_4$ , and  $\text{MnO}_2$ , were seen. With the starting composition  $\text{La}_y\text{MnO}_3$  ( $0.9 < y < 1$ ), the product crystallized in orthorhombic structure similar to  $\text{LaFeO}_3$ . Indexed patterns are shown in Figs. 1c and 1d.

Powder X-ray diffraction patterns of oxides grown in KCl melt are shown in Fig. 2 for various starting compositions  $\text{La}_y\text{MnO}_3$  ( $0.7 < y < 1$ ). Here also, for  $y < 0.9$ , the oxides crystallized in rhombohedral structure and for  $0.9 < y < 1$ , the oxides crystallized in orthorhombic structure. For the starting composition  $\text{La}_y\text{MnO}_3$  ( $y = 0.6$  and  $0.65$ ) with NaCl flux at  $900^\circ\text{C}$ ,  $\gamma$ - $\text{Mn}_2\text{O}_3$  impurity peaks were seen in the powder X-ray pattern. Thus, the lower limit of the starting composition for obtaining pure Na or K doped samples was  $y = 0.7$ . In Table 1, chemical composition, lattice parameters, cell volume per formula unit, electrical, and magnetic properties of the sodium doped lanthanum manganites are summarized. Similarly, the data on oxides grown in KCl melt for various starting compositions are given in Table 2.

The oxides synthesized from NaCl melt were doped with Na and the oxides grown in KCl melt contained K. As the La content increased, Na or K content decreased, demonstrating the substitution of Na or K in the La sites. For example, with the starting composition of  $\text{La}_{0.7}\text{MnO}_3$ , chemical composition of the oxide was  $\text{La}_{0.82}\text{Na}_{0.13}\text{Mn}_{2.93}$ , indicating both La (A site) and oxygen vacancies. Total

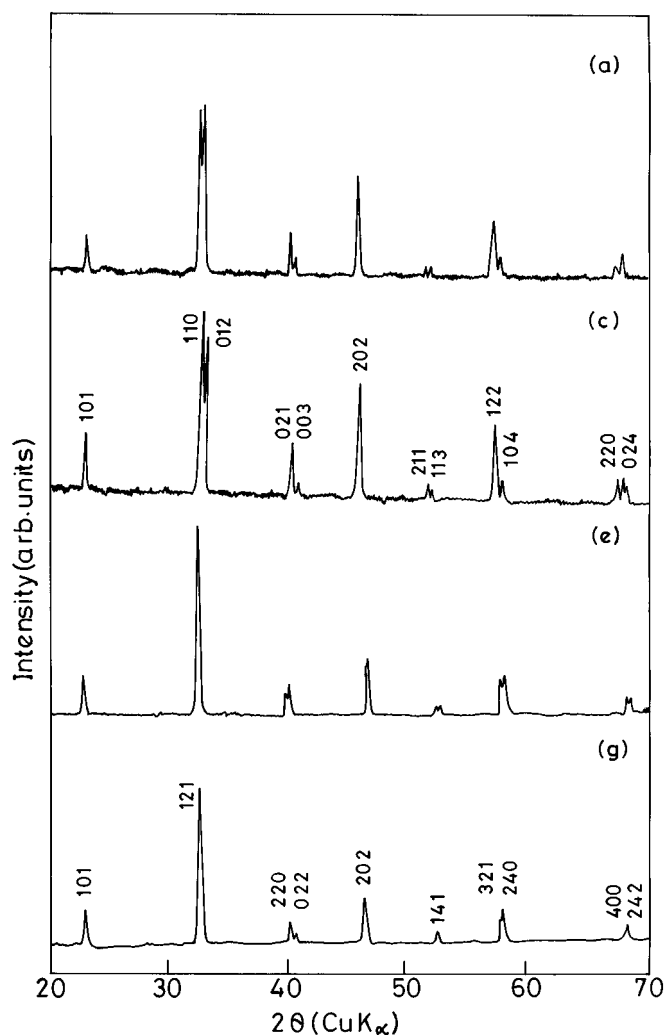


FIG. 1. Powder X-ray diffraction pattern of sodium-doped lanthanum manganites; curves (a), (c), (e), and (g) correspond to composition as in Table 1.

$\text{Mn}^{4+}$  content in this compound is 27%. For the initial La content  $y = 0.85$ , final composition was  $\text{La}_{0.91}\text{Na}_{0.09}\text{MnO}_3$ . Thus, stoichiometric  $\text{La}_{1-x}\text{Na}_x\text{MnO}_3$  could be prepared by NaCl flux method.

On increasing the starting lanthanum content, the compound crystallized in orthorhombic structure and no impurities peaks were detected in the X-ray diffraction. From the chemical analysis, we find that these oxides have Mn deficiency to the extent of 5–8%. The  $\text{Mn}^{4+}$  content was calculated from the composition, and it is in the range of 22–29%.

Typical scanning electron micrographs of the oxides crystallizing in rhombohedral and orthorhombic structure are shown in Figs. 3a and 3b. Energy dispersive X-ray analysis (EDAX) in the spot mode method confirms the presence of Na and K. A typical micrograph of sintered pellet in Fig. 3c

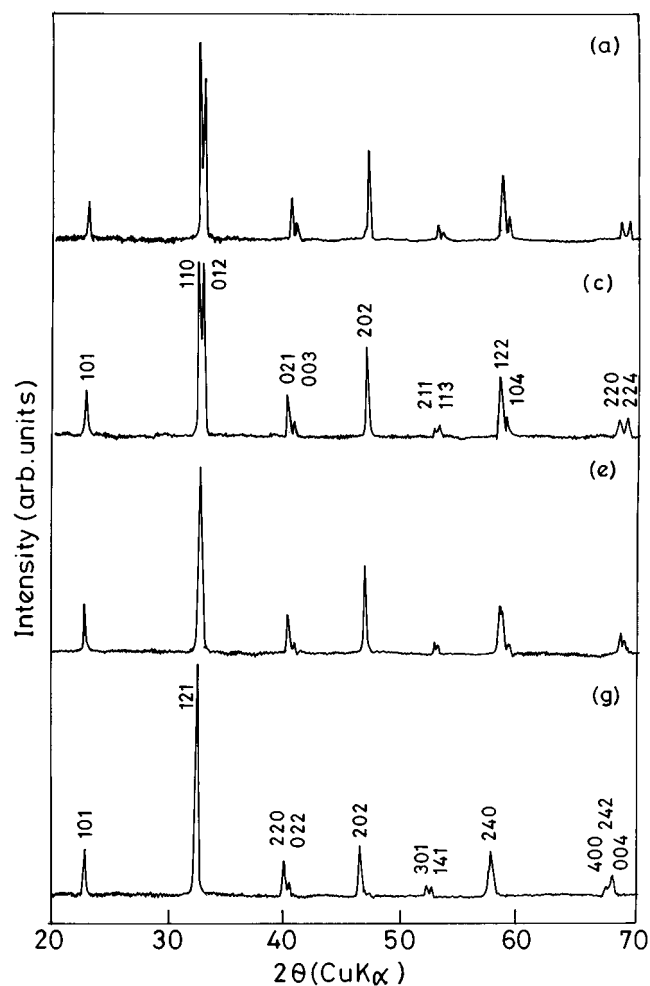


FIG. 2. Powder X-ray diffraction pattern of potassium-doped lanthanum manganites; curves (a), (c), (e), and (g) correspond to composition as in Table 2.

shows over 25% porosity. A comparison of composition from spot mode on large numbers of crystals and over a large area of the pellet showed that the samples are homogeneous.

Chemical analysis was carried out on the sintered materials also. Almost no variation in composition was observed on heating to 850°C in oxygen. Powder X-ray diffraction study of the oxygen-heated samples showed no variation in the case of parent oxides crystallizing in rhombohedral structure. However, oxides which crystallized in the orthorhombic structure transformed to rhombohedral structure on heating in oxygen. This is shown in Figs. 4a and 4b. Potassium doped samples also showed a similar transformation (Figs. 4c and 4d). No detectable impurity lines were seen in the powder pattern on heating the orthorhombic phases of Na and K doped samples.

### 3.1. Neutron Diffraction Studies

Neutron diffraction studies were done on two compositions among the series of oxides prepared here,  $\text{La}_{0.82}\text{Na}_{0.13}\text{MnO}_{2.93}$  and  $\text{La}_{0.82}\text{K}_{0.08}\text{MnO}_{2.89}$ . The diffraction patterns could be refined in  $R\bar{3}C$  space group. The occupancy parameters of La, Mn, and O were observed to exhibit strong correlations and hence were refined in

alternate cycles to minimize the effect of correlations. The proportion of La to Na (or K) at La sites was constrained to conform to the nominal composition. The Mn site indicated full occupancy and was fixed in the final cycle. The cell parameters, half width parameters, zero angle, and the scale factor were varied at all the cycles. A gaussian peak shape function was assumed. The refined parameters and bond distances are given in Table 3. Both La-site and O-site

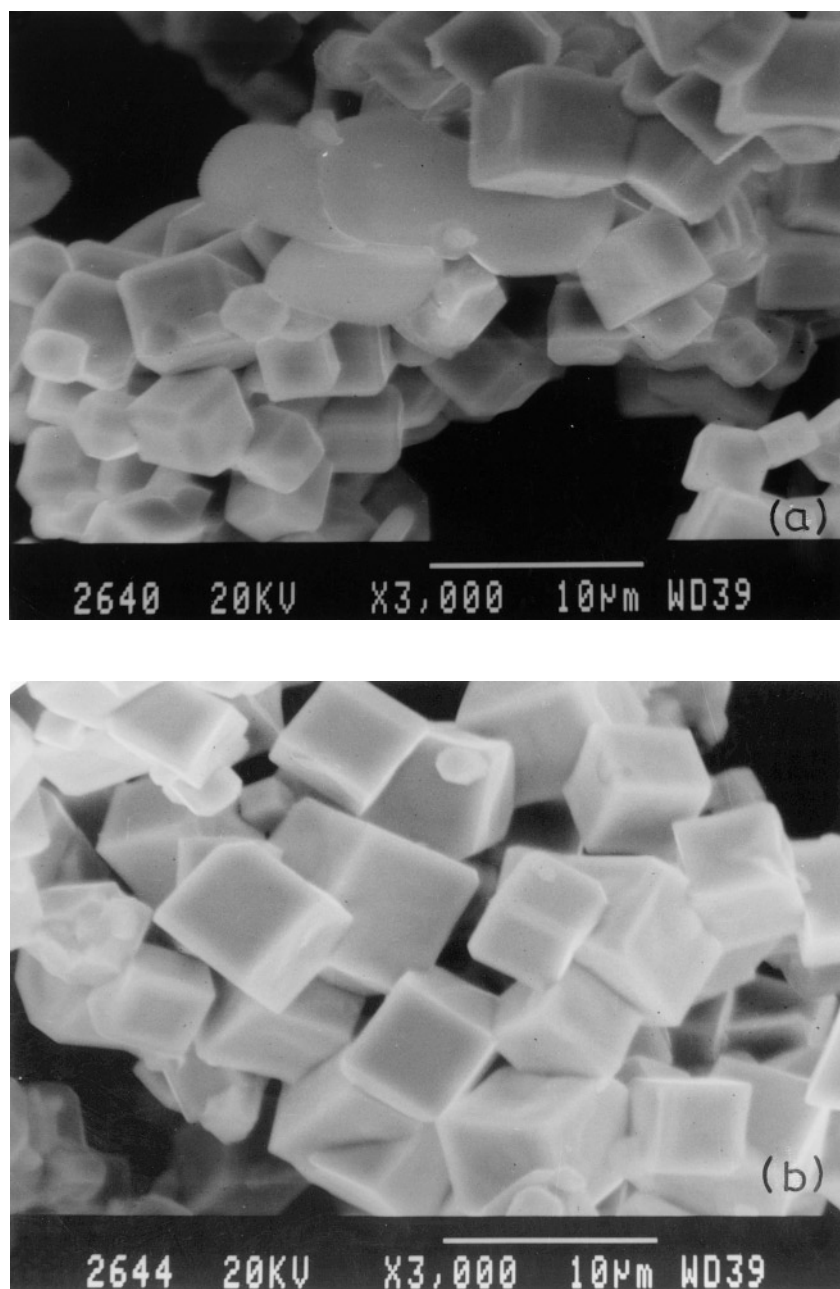


**FIG. 3.** Typical scanning electron micrographs (SEM) of (a)  $\text{La}_{0.85}\text{K}_{0.08}\text{MnO}_{2.93}$  (b)  $\text{La}_{0.99}\text{K}_{0.01}\text{Mn}_{0.92}\text{O}_{3.00}$ , and (c) sintered pellet of  $\text{La}_{0.82}\text{Na}_{0.13}\text{MnO}_{2.93}$  for porosity.

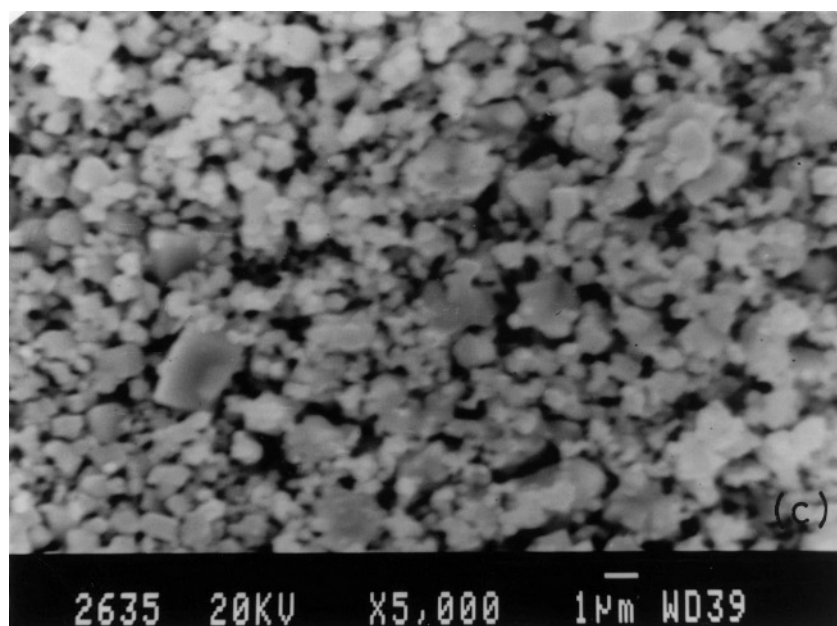


FIG. 3—Continued

vacancies are present. Refined cell parameters indicate larger lattice parameters for the K-substituted sample compared to the Na-substituted sample. The observed and calculated neutron diffraction patterns are shown in Figs. 5a and 5b. The refined composition of both the samples is in reasonable agreement with the chemical composition obtained earlier. The cell parameters agree well with the X-ray results.

### 3.2. Magnetic Properties

Magnetic susceptibility of Na doped oxides is shown in Fig. 6. The highest Curie temperature, 325 K, is seen for the

oxide having composition  $\text{La}_{0.82}\text{Na}_{0.13}\text{MnO}_{2.93}$ , and  $T_c$  decreases with an increase in La content or decrease in Na content. The inset shows the  $1/\chi$  vs  $T$  plot for the  $\text{La}_{0.98}\text{Na}_{0.02}\text{Mn}_{0.92}\text{O}_3$  phase. The  $1/\chi$  vs  $T$  in general showed Curie–Weiss behavior. In Fig. 7, susceptibility vs  $T$  plots of K doped samples are given. The highest  $T_c$  observed in this case is 310 K. The magnetic susceptibility measurements of oxygen-heated samples showed almost no variation in  $T_c$  in the case of oxides crystallized in rhombohedral structure. The oxides undergoing orthorhombic to rhombohedral structural transition showed a slight decrease in  $T_c$ , about 10 K. Tables 1 and 2 summarize  $\theta$  and  $T_c$  of these phases.

**TABLE 1**  
Composition, Lattice Parameters, and  $T_c$  of  $\text{La}_{1-x-y}\text{Na}_x\text{MnO}_{3-\delta}$  and  $\text{La}_{1-x}\text{Na}_x\text{Mn}_{1-z}\text{O}_3$  Phases Obtained from NaCl Melt

Starting La content $y$	Final composition <sup>a</sup>	Crystal structure	Lattice parameters ( $\text{\AA}$ ) <sup>b</sup>			Cell volume/ formula unit ( $\text{\AA}^3$ )	$\text{Mn}^{4+}$ content (%)	$T_{I-M}$ $\rho$ vs $T$	Transition temperature	
			$a$	$b$	$c$				$\theta$ (K)	$T_c$ (K)
(a) 0.70	$\text{La}_{0.82}\text{Na}_{0.13}\text{MnO}_{2.93}$	R	5.499	—	13.326	58.00	27	290	325	300
(b) 0.75	$\text{La}_{0.85}\text{Na}_{0.14}\text{MnO}_{2.97}$	R	5.488	—	13.316	58.00	25	280	310	280
(c) 0.80	$\text{La}_{0.90}\text{Na}_{0.09}\text{MnO}_{3.00}$	R	5.511	—	13.336	58.33	21	240	280	265
(d) 0.85	$\text{La}_{0.91}\text{Na}_{0.09}\text{MnO}_{3.00}$	R	5.511	—	13.318	58.33	18	225	—	—
(e) 0.90	$\text{La}_{0.97}\text{Na}_{0.03}\text{Mn}_{0.95}\text{O}_{3.00}$	O	5.511	7.767	5.477	58.50	22	Insulator	155	130
(f) 0.95	$\text{La}_{0.98}\text{Na}_{0.02}\text{Mn}_{0.93}\text{O}_{3.00}$	O	5.505	7.767	5.467	58.50	25	Insulator	150	125
(g) 1.00	$\text{La}_{0.98}\text{Na}_{0.02}\text{Mn}_{0.92}\text{O}_{3.00}$	O	5.506	7.767	5.474	58.25	29	Insulator	135	105

Note. R = Rhombohedral; O = Orthorhombic.

<sup>a</sup>The error in the analysis is  $\pm 0.01$ .

<sup>b</sup>Accurate within  $\pm 0.005$ .

**TABLE 2**  
**Composition, Lattice Parameters, and  $T_c$  of  $\text{La}_{1-x-y}\text{K}_x\text{MnO}_{3-\delta}$  and  $\text{La}_{1-x}\text{K}_x\text{Mn}_{1-z}\text{O}_3$  Phases Obtained from KCl Melt**

Starting La content $y$	Final composition <sup>a</sup>	Crystal structure	Lattice parameters ( $\text{\AA}$ ) <sup>b</sup>			Cell volume/ formula unit ( $\text{\AA}^3$ )	$\text{Mn}^{4+}$ content (%)	$T_{I-M}$ $\rho$ vs $T$	Transition temperature	
			$a$	$b$	$c$				$\theta$ (K)	$T_c$ (K)
(a) 0.70	$\text{La}_{0.82}\text{K}_{0.08}\text{MnO}_{2.89}$	R	5.516	—	13.324	58.33	24	250	310	300
(b) 0.75	$\text{La}_{0.85}\text{K}_{0.08}\text{MnO}_{2.93}$	R	5.519	—	13.336	58.66	23	240	300	290
(c) 0.80	$\text{La}_{0.91}\text{K}_{0.06}\text{MnO}_{3.00}$	R	5.526	—	13.362	59.00	21	210	280	260
(d) 0.85	$\text{La}_{0.93}\text{K}_{0.05}\text{MnO}_{3.00}$	R	5.529	—	13.354	59.00	16	140	—	—
(e) 0.90	$\text{La}_{0.97}\text{K}_{0.03}\text{Mn}_{0.95}\text{O}_{3.00}$	O	5.514	7.763	5.471	58.50	22	Insulator	195	180
(f) 0.95	$\text{La}_{0.98}\text{K}_{0.02}\text{Mn}_{0.93}\text{O}_{3.00}$	O	5.523	7.771	5.499	59.00	25	Insulator	145	125
(g) 1.00	$\text{La}_{0.99}\text{K}_{0.01}\text{Mn}_{0.92}\text{O}_{3.00}$	O	5.521	7.759	5.495	58.75	28	Insulator	130	105

Note. R = Rhombohedral; O = Orthorhombic

<sup>a</sup>The error in the analysis is less than  $\pm 0.01$ .

<sup>b</sup>Accurate within  $\pm 0.005$ .

### 3.3. Electrical Properties

Four probe electrical resistivity measurements as a function of temperature were done on the sintered pellets. In Fig. 8,  $\ln \rho$  vs  $T$  plots of sodium doped lanthanum manganites

are given. In the inset, a  $\rho$  vs  $T$  plot is given for the  $\text{La}_{0.85}\text{Na}_{0.14}\text{MnO}_{2.97}$  sample. In Fig. 9,  $\ln \rho$  vs  $T$  plots for the potassium doped oxides are given. The oxides crystallizing in the rhombohedral structures exhibit insulator-to-metal (I–M) transition as the temperature is decreased. This

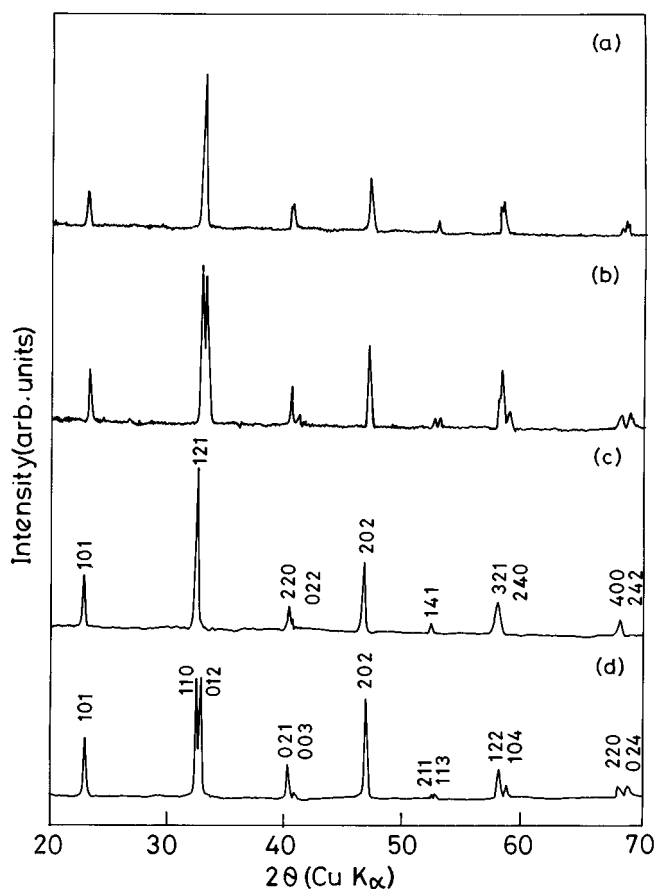


**FIG. 4.** Powder X-ray diffraction pattern of as-prepared sodium or potassium-doped oxide; curves (a)  $\text{La}_{0.98}\text{Na}_{0.02}\text{Mn}_{0.93}\text{O}_3$ , (b) after heating (a) at  $850^\circ\text{C}$ , (c)  $\text{La}_{0.98}\text{K}_{0.02}\text{Mn}_{0.93}\text{O}_3$ , and (d) after heating (c) at  $850^\circ\text{C}$ .

**TABLE 3**  
**Positional and Thermal Parameters (B) Obtained by Rietveld Refinement**

Atom	$\text{La}_{0.82}\text{Na}_{0.13}\text{MnO}_{2.93}$	$\text{La}_{0.82}\text{K}_{0.08}\text{MnO}_{2.89}$
La (0, 0, 0.25)		
B	0.5(1)	0.6(1)
N	0.79(1) / 0.12(1)	0.83(1) / 0.08(1)
Mn (0, 0, 0.5)		
B	0.5	0.5
N	1.00	1.00
O ( $x, 0, 0.25$ )		
X	0.4517(4)	0.4546(4)
B	1.06(7)	1.09(6)
N	2.81(2)	2.86(2)
Cell parameters ( $\text{\AA}$ )		
$a$	5.494(4)	5.515(5)
$c$	13.290(7)	13.396(9)
R factors		
$R_p$	3.76%	2.10%
$R_{wp}$	4.96	2.63
$R_{exp}$	3.16	2.23
Interatomic distances ( $\text{\AA}$ )		
La–O	$2.482(2) \times 3$	$2.507(2) \times 3$
La–O'	$2.737(1) \times 6$	$2.754(1) \times 6$
La–O''	$3.012(3) \times 3$	$3.008(1) \times 3$
Mn–O	$1.953(1) \times 6$	$1.960(1) \times 6$
Mn–O Bond valence	3.430	3.331

Note. The numbers in parentheses represent standard deviations referred to the last digit, and 100N denotes percentage occupancy.

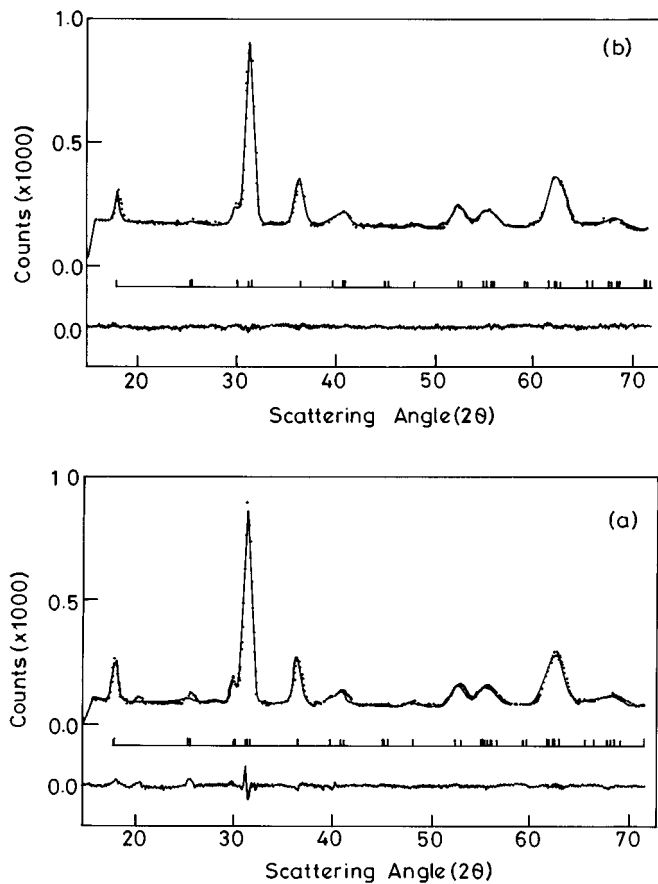


FIG. 5. Observed and calculated neutron diffraction patterns of (a)  $\text{La}_{0.82}\text{Na}_{0.13}\text{MnO}_{2.93}$  and (b)  $\text{La}_{0.82}\text{K}_{0.08}\text{MnO}_{2.89}$ .

behavior is similar to the divalent ion doped lanthanum manganites. I–M transition temperature is 30–60 K lower than the  $T_c$  observed from magnetic measurements. All the oxides with the starting composition  $\text{La}_y\text{MnO}_3$  ( $0.7 < y < 0.85$ ) showed I–M transition as well as para- to ferromagnetic transition. Oxides having Mn deficiency showed semiconducting behavior, even though  $\text{Mn}^{4+}$  content was in the range of 22–29%. Plots of  $\ln \rho$  vs  $1/T$  gave band gap in the range of 0.12 to 0.13 eV for these semiconducting phases.

#### 4. DISCUSSION

Na and K doped lanthanum manganites have been reported by Shimura *et al.* (13). They have prepared the sample by solid state method, and maximum substitution of Na for La in  $\text{LaMnO}_3$  is reported to be 0.2 with  $\text{Mn}^{4+}$  concentration as high as 40%. However, the highest  $T_c$  reported by them is 325 K, which agrees with the highest  $T_c$  observed here for an oxide having 27%  $\text{Mn}^{4+}$ . For  $\text{Mn}^{4+}$  concentration of 27%,  $T_c$  of 325 K is expected when we compare our results with the divalent ion doped lanthanum manganites (5).

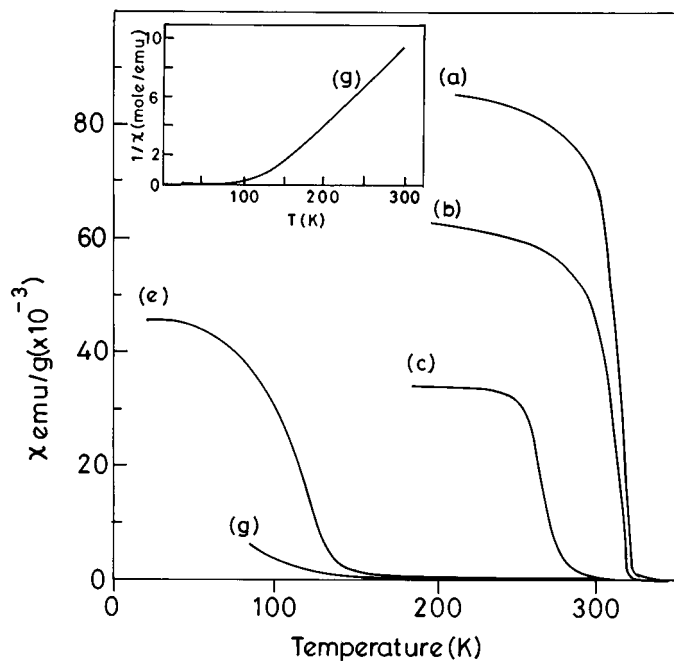


FIG. 6. Magnetic susceptibility as a function of temperature of sodium-doped lanthanum manganites measured at 1 K gauss field and 9 G gradient; curves (a), (b), (c), (e), and (g) correspond to composition as in Table 1. Inset shows  $1/\chi$  vs  $T$  for oxide (g) in Table 1.

Na and K doped lanthanum manganites made here can be classified into three categories:

(a) Those having both La- and oxygen-site vacancies showing ferromagnetic as well as insulator-to-metal transitions, (b) those having near-stoichiometric composition and still showing ferromagnetic and I–M transition, and (c) those which are Mn-deficient oxides showing ferromagnetic and semiconducting behavior.

A recent study of  $\text{La}_{1-y}\text{MnO}_3$  and  $\text{LaMn}_{1-z}\text{O}_3$  by Topfer and Goodenough (18) supports the formation of the three types of phases formed in NaCl or KCl fluxes. Partial occupancy of La by Na or K is observed here in this method of preparation. The compounds crystallizing in rhombohedral structure with the formula  $\text{La}_{1-x-y}\text{Na}_x\text{MnO}_{3-\delta}$  have both La and oxygen vacancies, and they showed ferromagnetic as well as metallic behavior. It may be mentioned here that oxygen deficiency does not alter the structure seen in  $\text{La}_{0.67}\text{Ba}_{0.33}\text{MnO}_{3-\delta}$  (11) and  $\text{La}_{0.6}\text{Pb}_{0.4}\text{MnO}_{3-\delta}$  (12). Thus, both A-site and oxygen vacancy can be accommodated in this structure. For a narrow range of initial composition  $\text{La}_y\text{MnO}_3$  ( $y = 0.85 \pm 0.05$ ) near-stoichiometric  $\text{La}_{1-x}\text{A}_x\text{MnO}_3$  ( $A = \text{Na}, \text{K}$ ) phases are indeed formed in NaCl or KCl fluxes. They do show ferromagnetic transition as well as I–M transition. In the case of oxides precipitated in the orthorhombic structure with starting composition  $\text{La}_y\text{MnO}_3$  ( $0.9 < y < 1$ ), the oxides

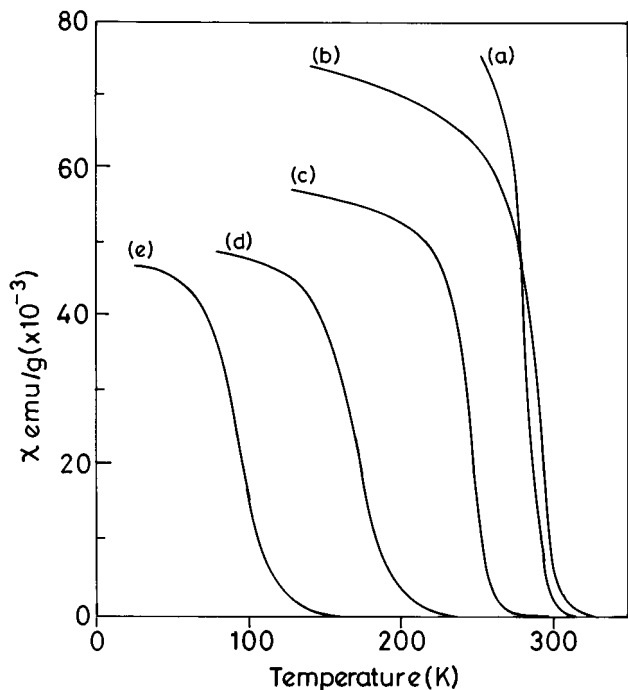


FIG. 7. Magnetic susceptibility as a function of temperature of potassium-doped lanthanum manganites measured at 1 K gauss field and 9 G gradient; curves (a), (b), (c), (e), and (g) correspond to composition as in Table 2.

gave 5–8% Mn deficiency.  $\text{Mn}^{4+}$  content was as high as 29% (see Tables 1 and 2). Ferromagnetic and insulating properties of such Mn-deficient oxide has been discussed in

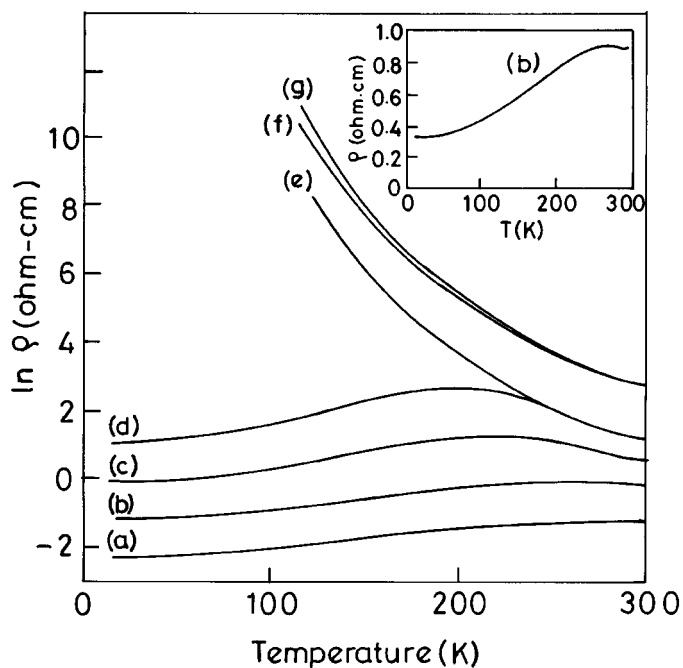


FIG. 8. Plots of  $\ln \rho$  vs  $T$  of sodium-doped lanthanum manganites; curves (a), (b), (c), (d), (e), (f), and (g) correspond to composition as in Table 1. In the inset,  $\rho$  vs  $T$  plot of curve (b) in Table 1.

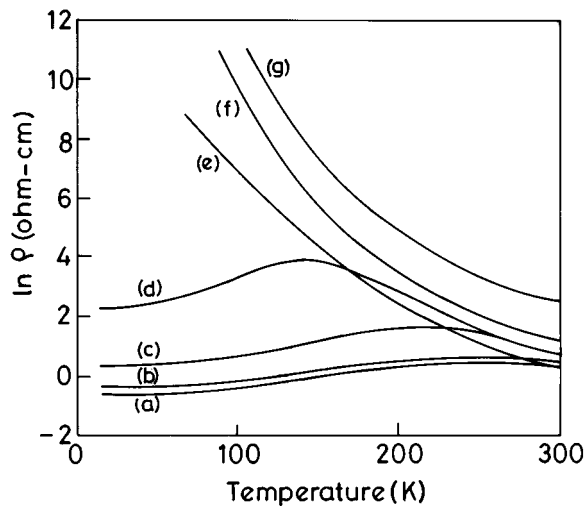


FIG. 9. Plots of  $\ln \rho$  vs  $T$  of potassium-doped lanthanum manganite; curves (a), (b), (c), (d), (e), (f), and (g) correspond to composition as in Table 2.

detail by Topfer and Goodenough. They have suggested that the trapping of holes in Mn sites is the reason for the insulating behavior. It is interesting to find that these Mn-deficient oxides have  $T_c$  close to the values reported by them. Therefore, the flux method can be employed to make La site- as well as Mn site-deficient oxides by varying the La:Mn starting ratio.

The origin of orthorhombic to rhombohedral structural transition when the ferromagnetic insulating oxides are heated in oxygen or air at  $850^\circ\text{C}$  is not clear to us. One possibility is that further oxidation of  $\text{Mn}^{3+}$  to  $\text{Mn}^{4+}$  on heating may take place. This could create vacancy in the La site. Careful analysis and structural studies are needed to confirm this.

## 5. CONCLUSION

Sodium or potassium doped lanthanum orthomanganites have been grown in NaCl or KCl melts at relatively low temperatures for the first time. Maximum Na content substituted for La was 0.13, and K was 0.08. The compounds have typical composition  $\text{La}_{1-x-y}\text{Na}_x\text{MnO}_{3-\delta}$ , with both La and oxygen deficiencies. The highest  $T_c$  of Na-doped oxide was 325 K, and K-doped oxide was 310 K. Neutron diffraction studies supported the formation of such phases crystallizing in  $R\bar{3}C$  space group. The oxides crystallizing in rhombohedral structure with A-site vacancy and  $\text{Mn}^{4+}$  content greater than 18% show insulator-to-metal transition coupled with para- to ferromagnetic transition. Oxides crystallizing in orthorhombic structure with Mn-site vacancy and 24–29%  $\text{Mn}^{4+}$  content are ferromagnetic insulators only.



## ACKNOWLEDGMENTS

We thank IUC/DAEF, Indore and Department of Science and Technology, Government of India for financial assistance.

## REFERENCES

1. G. H. Jonker and J. H. Van Santen, *Physica* **16**, 337 (1950).
2. E. O. Wollan and W. C. Koehler, *Phys. Rev.* **100**, 545 (1955); G. H. Jonker, *Physica* **22**, 707 (1956).
3. R. Von Helmolt, J. Wecker, B. Holzapfel, L. Schultz, and K. Samwer, *Phys. Rev. Lett.* **71**, 2331 (1993).
4. K. Chahara, T. Ohno, M. Kasai, and Kozono. *Appl. Phys. Lett.* **63**, 1990 (1993).
5. H. L. Ju, C. Kwon, Q. Li, R. L. Greene, and T. Venkatesan, *Appl. Phys. Lett.* **65**, 2108 (1994).
6. S. S. Manoharan, Dhananjay Kumar, M. S. Hegde, K. M. Satyalakshmi, V. Prasad, and S. V. Subramanyam, *J. Appl. Phys.* **76**, 3923 (1994).
7. J. S. Zhou, W. Archibald, and J. B. Goodenough, *Nature* **381**, 770 (1996).
8. M. A. Subramanyan, B. H. Toby, A. Pramirez, W. J. Marshall, A. W. Sleight, and G. H. Kwei, *Science* **273**, 81 (1996).
9. J. B. Goodenough, *Prog. Solid State Chem.* **5**, 145 (1971).
10. S. Sundar Manoharan, Dhananjay Kumar, M. S. Hegde, K. M. Satyalakshmi, V. Prasad, and S. V. Subramanyam, *J. Solid State Chem.* **117**, 420 (1995).
11. H. L. Ju, J. Gopalakrishnan, I. L. Peng, Q. Li, G. C. Xiong, T. Venkatesan, and R. L. Greene, *Phys. Rev. B* **51**, 6143 (1995).
12. K. M. Satyalakshmi, S. Sundar Manoharan, M. S. Hegde, V. Prasad, and S. V. Subramanyam, *J. Appl. Phys.* **78**, 6861 (1995).
13. Tetsuo Shimura, Toshimasa Hayashi, Yoshiyuki Inaguma, and Mitsuru Itoh, *J. Solid State Chem.* **124**, 250 (1996).
14. M. Sahana, R. N. Singh, C. Shivakumara, N. Y. Vasanthacharya, M. S. Hegde, S. Subramanian, V. Prasad, and S. V. Subramanyam, *Appl. Phys. Lett.* **70**, 2909 (1997).
15. D. B. Wiles and R. A. Young, *J. Appl. Crystallogr.* **14**, 149 (1981).
16. I. G. Krogh Andersen, E. Krogh Andersen, P. Norby, and E. Skou, *J. Solid State Chem.* **113**, 320 (1994).
17. A. I. Vogel, "Textbook of Quantitative Chemical Analysis," 5th ed., p. 584, Longman, England, (1989).
18. J. Topfer and J. B. Goodenough, *Chem. Mater.* **9**, 1467 (1997).